Carbohydrate Polymers 115 (2015) 422–431

Contents lists available at ScienceDirect

Carbohydrate Polymers

journal homepage: www.elsevier.com/locate/carbpol

# Rheological and structural characterization of HA/PVA-SbQ composites film-forming solutions and resulting films as affected by UV irradiation time

Huiyu Bai [a,*], Yunlong Sun [b], Jing Xu [c], Weifu Dong [a], Xiaoya Liu [a]

[a] The Key Laboratory of Food Colloids and Biotechnology, Ministry of Education, School of Chemical and Material Engineering, Jiangnan University, Wuxi, Jiangsu 214122, China
[b] School of Materials Science and Engineering, East China University of Science and Technology, Shanghai 200237, China
[c] Patent Examination Cooperation Jiangsu Centre of the Patent Office, State Intellectual Property Office, Suzhou, Jiangsu 215011, China

ARTICLE INFO

*Article history:*
Received 3 May 2014
Received in revised form 3 August 2014
Accepted 21 August 2014
Available online 16 September 2014

*Keywords:*
Hyaluronan acid
PVA-SbQ
Photo-crosslinking
Composites film
Packaging material

ABSTRACT

Hyaluronan (HA)/poly (vinyl alcohol) bearing styrylpyridinium groups (PVA-SbQ) composites film-forming solutions were prepared by a negatively charged HA and an oppositely charged PVA-SbQ. The rheological properties and structural characterization of HA/PVA-SbQ composites in aqueous solution were investigated. Zeta potential measurements and TEM were utilized to explore the formation of HA/PVA-SbQ complex micelles in aqueous solution. UV spectra and DLS experiments confirmed that the micelles are photo-crosslinkable. HA/PVA-SbQ composites films were prepared by a casting method. The microstructure and properties of the film were analyzed by SEM, optical transmittance, DSC, XRD and tensile testing. The crosslinked HA/PVA-SbQ composites films exhibited higher UV light shielding and visible light transparency and better mechanical and water vapor barrier properties as well as thermal stability than the uncrosslinked HA/PVA-SbQ composites films, indicating the formation of three-dimensional network structure. This work provided a good way for increasing the mechanical, thermal, water vapor barrier, and optical properties of HA materials for the packaging material.



## 1. Introduction

In recent years, the food and packaging industries have been joining their efforts to determine new ways to protect food from environmental conditions and mechanical stresses (Ghasemlou, Khodaiyan, & Oromiehie, 2011).

Polysaccharides used to prepare packaging material include hyaluronan acid (HA), chitosan (CS), cellulose derivatives, starch and pectin. They are preferred because of their high film forming ability. HA is a naturally occurring polysaccharide originally extracted from bovine vitreous humor, rooster combs or umbilical cords (Rinaudo, 2008a,b), and now has been successfully produced on a larger scale by streptococcus bacteria in high purity and good yield (Gao, Du, & Chen, 2006; Ogrodowski, Hokka, & Santana, 2005). It consists of repeating β-(1→4)-D-glucuronic acid β-(1→3)-N-acetyl-D-glucosamine disaccharide units (Chytil & Pekar, 2009; Cowman & Matsuoka, 2005). HA is an attractive materials building block for its hybiocompatiblity with biomedicine and pharmaceutics application (Lee, Ahn, & Park, 2009; Lee, Lee, & Park, 2008; Pitarresi, Pierro, Palumbo, Tripodo, & Giammona, 2006; Vázquez et al., 2009), and HA film is a promising packaging material. However, HA packaging films exhibit several disadvantages such as strong hydrophilic character and poor mechanical properties, compared with synthetic packaging films. Therefore, in order to obtain the best physical and mechanical properties for HA based film, the modifications such as crosslinking with other biomolecules become imminent in application.

HA derivative cross-linked can be prepared at room temperature (RT) in conditions slightly alkaline or acidic (Barbucci et al., 2002; Bulpitt & Aeschlimann, 1999). Additionally, such reactions employed small molecular crosslinking reagents, often in large excess, which required considerable purification in order to obtain materials for physiological use (Luo, Kirker, & Prestwich, 2000).

We describe herein a new HA based film well-suited to packaging films. It was prepared by mixing HA and a macro-molecular crosslinker, which is a poly (vinyl alcohol) bearing a styrylpyridinium groups residue as its photosensitive group (PVA-SbQ) (Scheme 1) (Ichimura & Watanabe, 1980), under UV irradiation condition. PVA-SbQ has been widely used as a photocrosslinkable material due to its water stability, high photosensitivity and

* Corresponding author. Tel.: +86 13382888306.
*E-mail address:* bhy.chem@163.com (H. Bai).

http://dx.doi.org/10.1016/j.carbpol.2014.08.103
0144-8617/

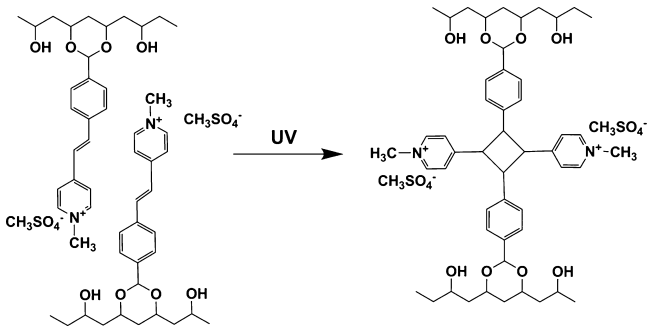


**Scheme 1.** Chemical structures of PVA-SbQ and its photo-dimerization mechanism.

good storage stability (Ichimura & Watanabe, 1982). The photocrosslinking behavior and mechanism of PVA-SbQ have been systematically investigated by Ichimura (Ichimura, 1996; Ichimura & Watanabe, 1982), Shindo (Shindo, Hasegawa, Kawanobe, & Inoue, 2001; Shindo, Morikawa, Hasegawa, Sugimura, & Adachi, 1995; Shindo, Yamada, Kawanobe, & Inoue, 2002) and Cockburn (Cockburn, Davidson, & Pratt, 1996). The styrylpyridinium (SbQ) moiety is photoreactive and forms a dimer on UV irradiation (Scheme 1) (Ichimura & Watanabe, 1980, 1982). This photocrosslinkable polymer PVA-SbQ has found its use in nanofibers, gels, etc. (Hertzberg, Moen, Vogelsang, & Østgaard, 1995; Liu, Bolger, Cahill, & McGuinness, 2009).

The anionic polyelectrolyte character of HA can form electrostatic complexes with the cationic character of PVA-SbQ, and the combination of HA and PVA-SbQ may have beneficial effects on the mechanical and thermal properties and hybiocompatiblity of HA/PVA-SbQ composites film as a potential packaging film. This new biocompatible material can be used directly in any system without purification, since it only contains two biocompatible polymers (Tao, Ai, Bai, & Liu, 2012).

In order to make a good film or leveling coating on solid surface, the viscosity of film-forming solutions should be suitable which can prevent sagging by gravity effects and allow capillary leveling (Peressini, Bravin, Lapasin, Rizzotti, & Sensidoni, 2003). It is noted that rheological properties, which are sensitive to variations in molecular structure, are useful in developing structure–function relationships for systems of polysaccharide solutions (Xu, Liu, & Zhang, 2006). Therefore, the knowledge of the film-forming solutions (FFS) rheological properties by dynamic test is important for the design and processing of films by casting. Moreover, the desired mechanical properties of packaging film depend on viscoelastic properties of FFS. It may be found in the specialized literature that diverse studies on the rheological behavior, including the viscoelasticity, have been carried out with relatively highly viscous FFS (Pires & Santana, 2011; Rinaudo, 2008a,b). However, few studies have been carried out about the characterization of low viscosity

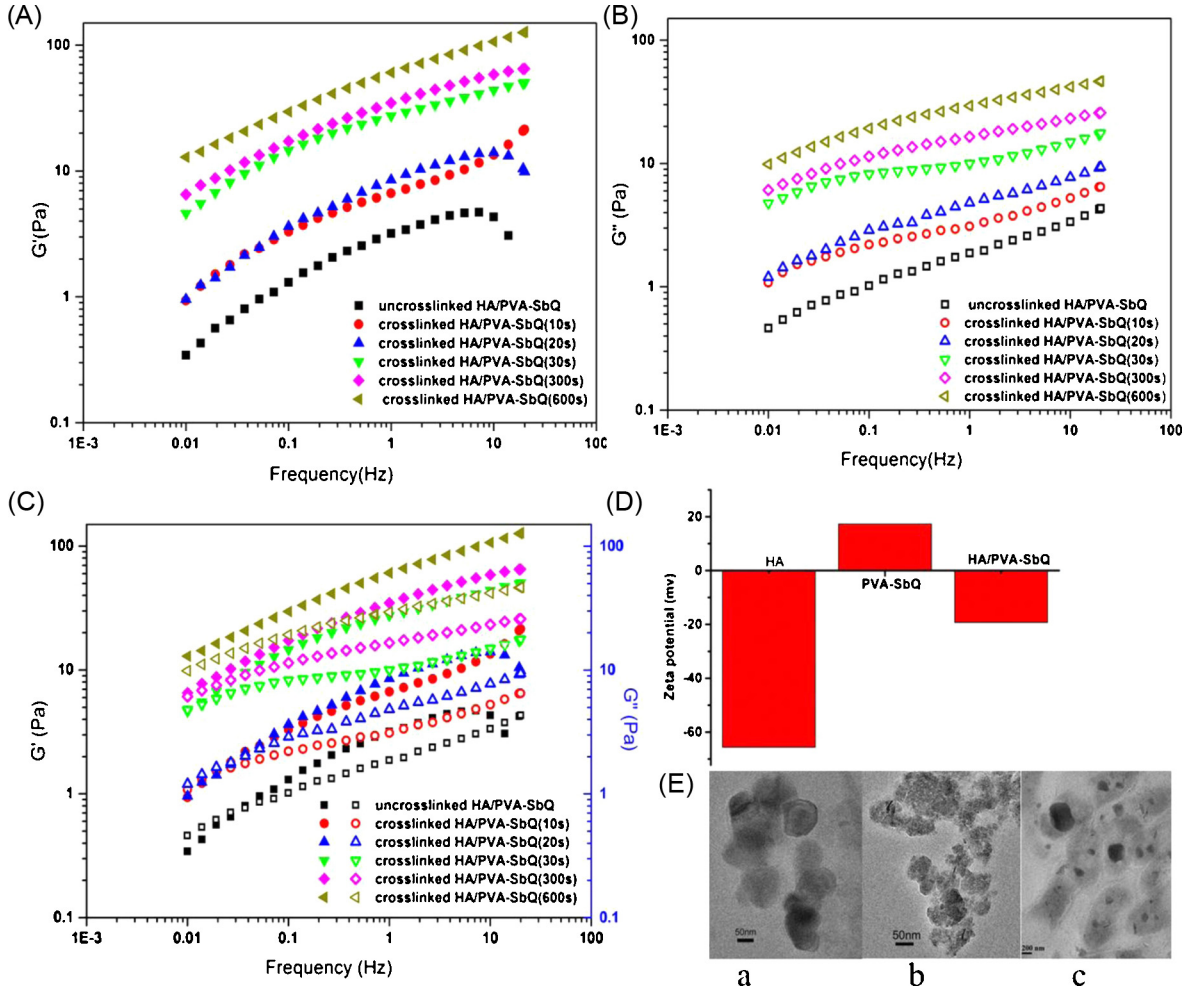


**Fig. 1.** Storage modulus ($G'$) and loss modulus ($G''$) (A–C) as a function of frequency for HA/PVA-SbQ composites solution with different UV irradiation time; The dependence of the Zeta-potential of HA, PVA-SbQ and HA/PVA-SbQ composite solutions (D); TEM image of HA (E: a), PVA-SbQ (E: b), and HA/PVA-SbQ composite solution without UV irradiation (E: c).

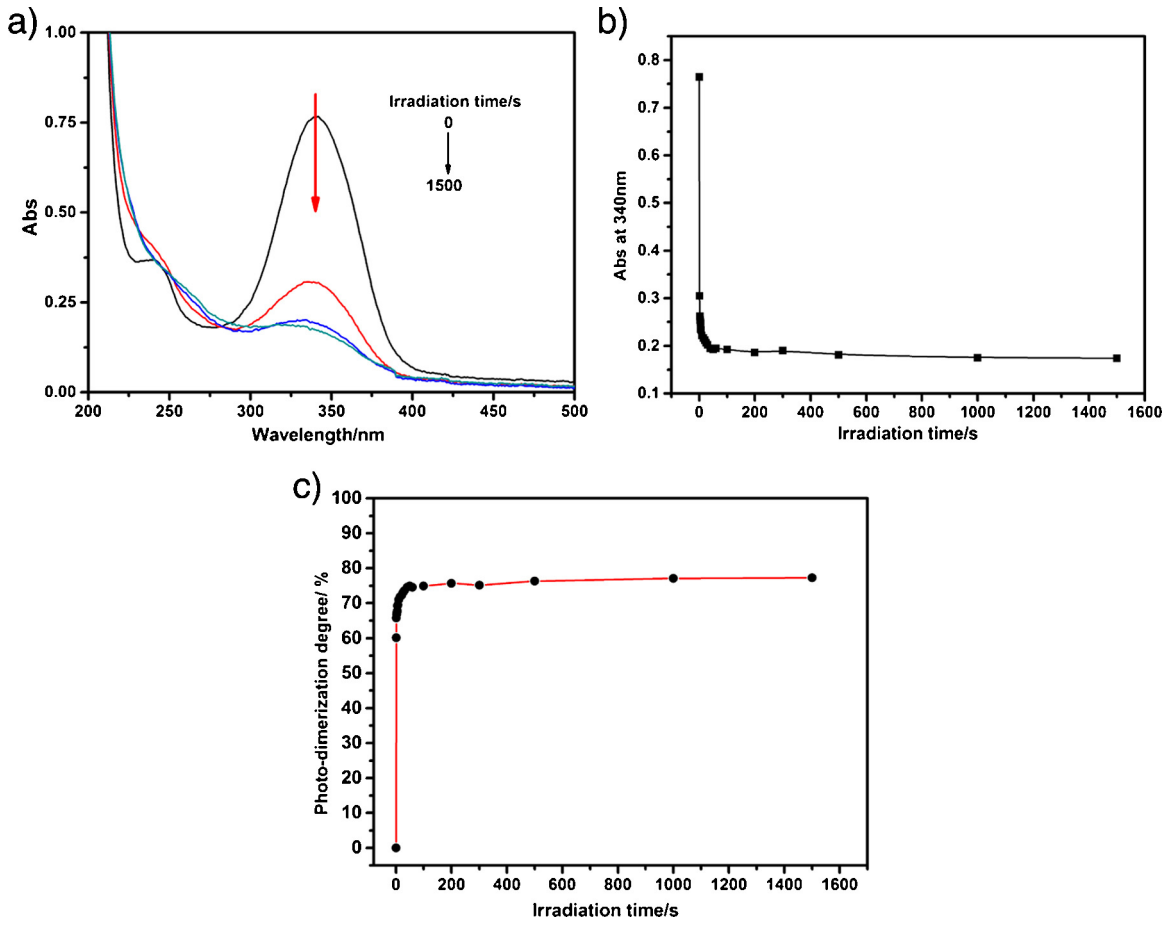


**Fig. 2.** UV absorption spectra (a), UV absorption at around 340 nm (b), and photo-dimerization degree (c) of the HA/PVA-SbQ composite solution radiated at different irradiation time.

FFS, produced usually with low concentration of macromolecules. Within this context, the purpose of this work was to evaluate the effect of UV irradiation time on the rheological of relatively low viscosity HA/PVA-SbQ FFS and structure of HA/PVA-SbQ complex in aqueous solution, and the mechanical and thermal and water vapor barrier properties of the resulting films. These results are very important for evaluating such films' possible applications as packaging material.

## 2. Materials and methods

### 2.1. Materials

HA, with a molecular weight of 210 kDa, was purchased from Zhenjiang Dongyuan Biology Technology Co., Ltd. (China). PVA-SbQ ($M_w$ = 45,000 and 4.1 mol% SbQ content) was purchased from Shanghai KOKI Co., Ltd. (China). The chemicals were used as received without further purification. Deionized water was used for the preparation of all solutions.

### 2.2. Preparation of HA/PVA-SbQ composites film-forming solution

HA was dissolved into water to prepare a HA (1 wt%) solution. Stock solutions of PVA-SbQ (1 wt%) were prepared by dissolving PVA-SbQ in water. The HA solutions were mixed with PVA-SbQ solution in equal volume to prepare the film-forming solutions using a magnetic stirrer for 15 min and the resulting solutions were irradiated under a POWER ARC UV 100 Lamp ($\lambda_{max}$ = 500 nm). HA/PVA-SbQ composites FFS with different UV irradiation time (0, 10, 20, 30, 300, 600 s) were obtained. All the mixtures were stored in glass bottles wrapped in aluminum foil package prior to use.

### 2.3. Characterization of HA/PVA-SbQ composites film-forming solution

The rheological tests were carried out on a rotational AR-G2 rheometer with a diameter of 40 mm cone-plate geometry. Oscillatory shear was applied on the sample at a constant temperature 25 °C. The strain amplitude is 2% in all experiments. Transmission electron microscopy (TEM) was performed on a JEOL JEM-2100 microscope, operating at an acceleration voltage of 200 kV. The samples were prepared by drop-coating the micelle solution on the carbon-coated copper grid and drying at room temperature before observation. Zeta-potentials of the micelle solutions were measured by a Malvern Zetasizer 2000 instrument. The solution samples were injected into the instrument and the zeta-potential measurement was carried out at room temperature. The absorbance of HA/PVA-SbQ composites film-forming solution from a wavelength of 200 to 800 nm was measured by TU-1901 UV–vis spectrophotometer. Dynamic light scattering (DLS) measurements were carried out using an ALV-5000 laser light scattering spectrometer. All the solution samples were filtered through 0.45 μm Millpore filters to remove dust before the light scattering measurements. DLS measurements were performed at a fixed scattering angle of 90° at 25 °C. The apparent hydrodynamic radius $R_h$ was obtained using the CONTIN program.

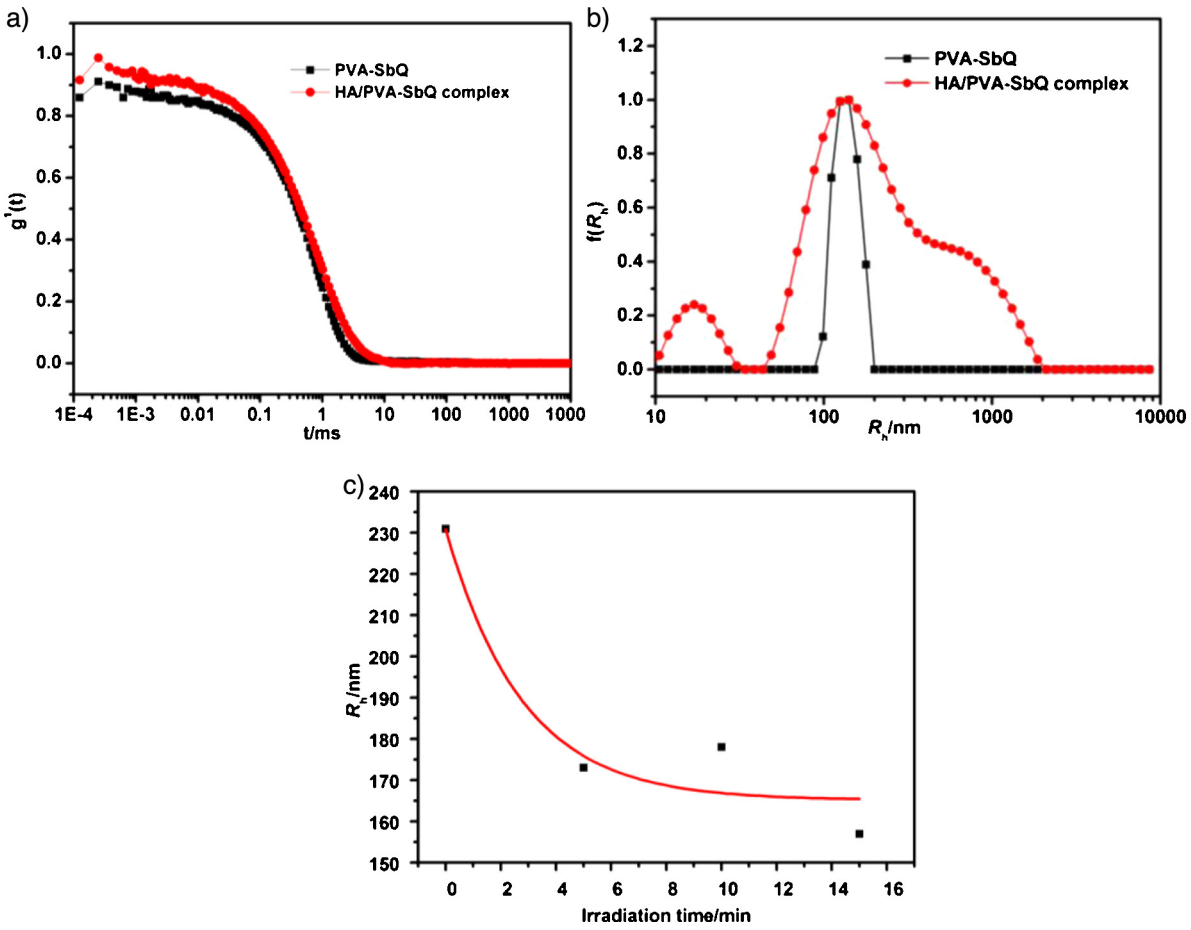


**Fig. 3.** Correlation function $g^1(t)$ (a), the corresponding $f(R_h)$ (b) for PVA-SbQ and HA/PVA-SbQ composite solutions and effect of UV irradiation time on $R_h$ (c) of HA/PVA-SbQ composite solutions.

### 2.4. Preparation of HA/PVA-SbQ composites films

HA/PVA-SbQ composites films were cast by pouring HA/PVA-SbQ composites FFS with different UV irradiation time (0, 10, 20, 30, 300, 600 s) onto glass plates resting on a leveled surface for approximately 24 h at 40°C in oven. Dried films were peeled off the casting surface and stored inside desiccators at 25 ± 1 °C until evaluation. Saturated magnesium nitrate solution (50% RH) was used to meet required relative humidity.

### 2.5. Determination of mechanical and thermal as well as water vapor barrier properties of HA/PVA-SbQ composites films

Tensile strength (TS) and elongation at break (EB) of the HA/PVA-SbQ composites films were measured on a WDT-10 universal testing machine with a tensile rate of 5 mm/min according to ISO527-3:1995 (E). An average value from five replicates of each sample was taken.

Thermal property of the HA/PVA-SbQ composites films was examined using a differential scanning calorimetry (DSC) (DSC1 Metter-Toledo, Switzerland). Approximately 5 mg HA/PVA-SbQ composites films were tested at a heating rate of 10 °C/min between 0 and 250°C under nitrogen atmospheres.

Water vapor barrier property of the HA/PVA-SbQ composites films was determined by measuring water vapor transmission rate (WVTR) and water vapor permeability (WVP). WVTR of the pure HA and HA/PVA-SbQ composite films was measured according to modified ASTM E96 method ( Ou, Kwok, & Kang, 2004). Briefly, film specimens were clamped on the top of glass bottles with diameter of 3 cm and depth of 5 cm containing 3 g anhydrous calcium chloride ($CaCl_2$) to maintain 0% RH inside the bottle, followed by sealing the film over the edge of bottle with applying molten paraffin. Then the bottles were stored under the desiccator with a relative humidity of 75% at 30 °C. The RH was maintained by placing 500 mL of saturated sodium chloride (NaCl) solution in the bottom of the desiccator. The bottles were weighed every 12 h for 5 days. The amount of water permeated through the films was determined from the weight gain of the bottles. Both WVTR and WVP were calculated according to (Tomé et al., 2011):

$$\mathrm{WVTR} = \frac{\Delta W}{\Delta t \cdot A} \quad (1)$$

$$\mathrm{WVP} = \frac{\mathrm{WVTR} \cdot L}{\Delta P} \quad (2)$$

where WVTR was in g/(h m$^2$), $\Delta W/\Delta t$ was rate of water gain in g/h, $A$ was the exposed area of the film in m$^2$, $L$ was the mean thickness of samples in m, and $\Delta P$ was the difference in partial water vapor pressure between the two sides of film samples in Pa. The water vapor pressure on the high-stream side of the film was 3.2 kPa (water vapor pressure of saturated NaCl aqueous solution at 30 °C), while the low-stream side was assumed to be zero.

### 2.6. Characterization of HA/PVA-SbQ composites films

The optical transmittance of the HA/PVA-SbQ composites films were measured with a TU-1901 UV-visible spectrophotometer from a wavelength of 200 to 800 nm. SEM images of the surface of HA/PVA-SbQ composites films was performed on a Hitachi

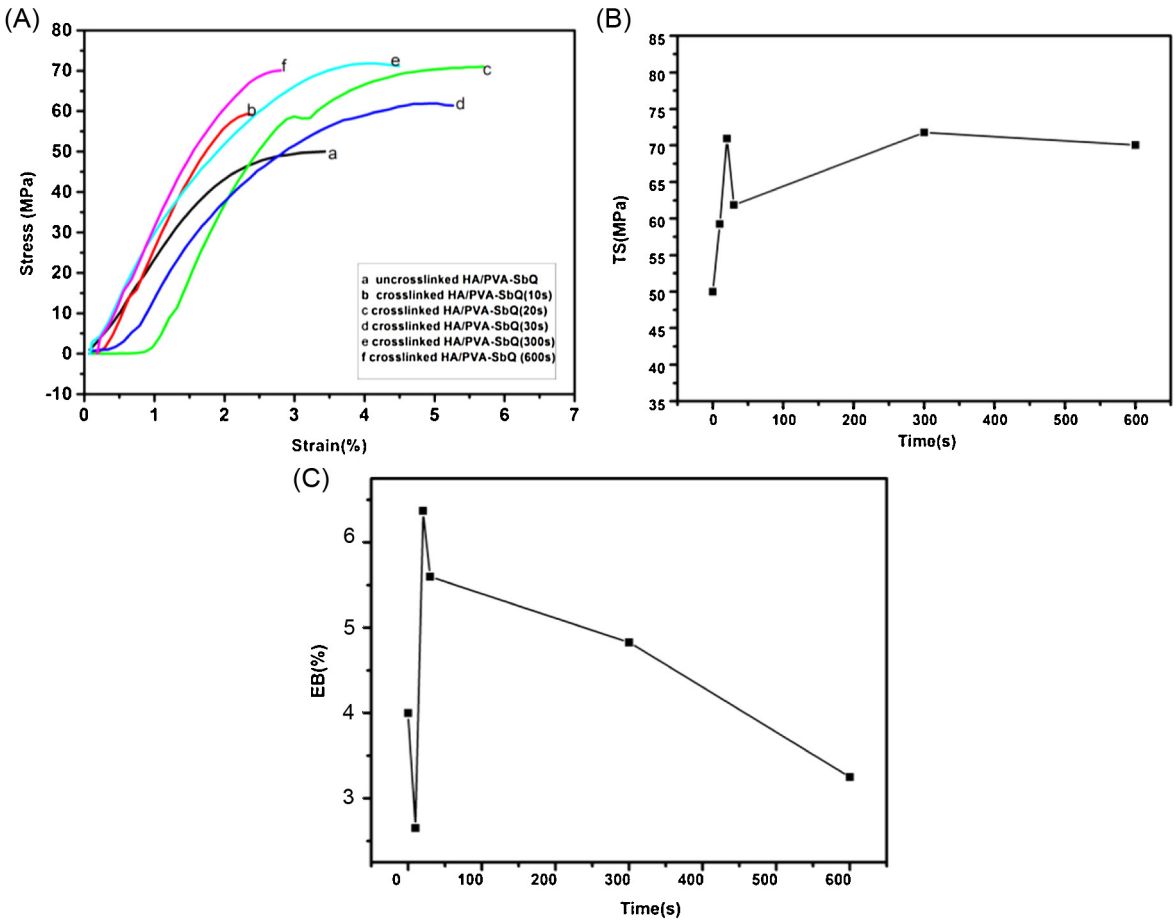


**Fig. 4.** Tensile stress–strain curves (A) and the effect of UV irradiation time on the TS (B) and EB (C) for HA/PVA-SbQ composites films.

S-4800 scanning electron microscope. X-ray diffractograms of film samples were derived using a Rigaku D/MAX2550 diffractometer with Cu Kα radiation. The samples were exposed to an X-ray beam, the X-ray generator running with radiation Cu Kα ($\lambda = 1.542$ Å). The relative intensity was recorded at ambient temperature over an angular range ($2\theta$) of 30–70° at a rate of 2°/min.

## 3. Results and discussion

### *3.1. Rheological and structural characterization of HA/PVA-SbQ composites FFS*

#### *3.1.1. Rheological behavior*

The rheological analysis is a useful tool to explore relationships between mechanical behavior and structure, concentration, and molecular weight of biopolymers solutions (Chamberlain & Rao, 2000). Therefore, the rheological behaviors are of decisive importance for all applications and rheological properties provides valuable indications to better design proper substitutes for specific packaging application (Ambrosio, Borzacchiello, Netti, & Nicolais, 1999).

The leveling of irregularities in liquid coating (or in FFS casting) depends mainly on their rheological properties (Lafargue, Lourdin, & Doublier, 2007). According to Cuq (Cuq, Aymard, Cuq, & Guilbert, 1995), to cast a high viscosity FFS is difficulty and needs a dispersing machine (spreader). Nevertheless, the FFS studied in this work had low viscosity values, which readily allowed casting these solutions by free flow.

Dynamic frequency sweep tests were performed in the linear viscoelastic range to determine the frequency dependence of the storage modulus ($G'$) and loss modulus ($G''$). Fig. 1(A–C) showed the viscoelastic behavior of photo-crosslinked HA/PVA-SbQ composites solution with different UV irradiation time. As shown in Figure 1A, B, C it was observed a trend of increasing the $G'$ and $G''$ values as the frequency increased in photo-crosslinked HA/PVA-SbQ composites solution with different UV irradiation time. Furthermore, in HA/PVA-SbQ composites solution, increases of $G'$ and $G''$ values as the UV irradiation time increased were observed. Since the storage modulus usually represents the elastic character and the loss modulus describes the viscous behavior, these results suggest that enhancement in structural entanglement increases the $G'$ modulus, while structural breakdown increases the $G''$ modulus (Rwei, Chen, Mao, & Fang, 2008). Although $G'$ and $G''$ values were similar, the $G'$ were slightly greater than the $G''$ (in Fig. 1C), indicating that more elastic systems were obtained. These high $G'$ values are due to a loose network created by intermolecular electrostatic interaction between HA and PVA-SbQ. With the UV irradiation time increasing, chemical cross-linking that is the result of the dimerization of SbQ moieties of PVA-SbQ takes place. This causes that HA/PVA-SbQ composites solution were more solid than liquid. Similar results have been observed in works on film forming solutions based on gelatin and poly (vinyl alcohol) blends (Moraes, Carvalho, Bittante, Solorza-Feria, & Sobral, 2009). These suggested that the mechanism of cross-linkage in HA/PVA-SbQ composites solution is based on the electrostatic interaction between negatively charged HA and cationic sites in PVA-SbQ and the dimerization of SbQ moieties of PVA-SbQ.

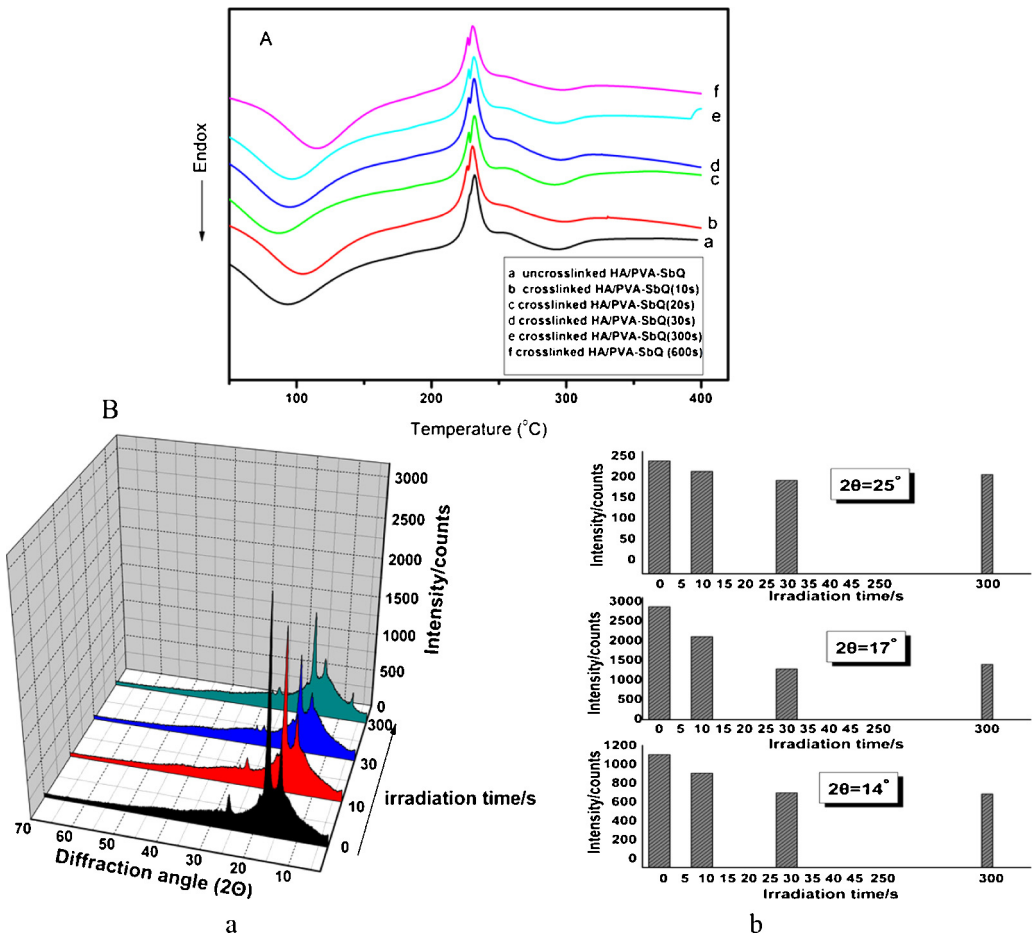


**Fig. 5.** DSC thermograms (A), X-ray scans (B: a) and different peaks intensity ($2\theta = 14°$, 17°, 25°) (B: b) of HA/PVA-SbQ composites films with different UV irradiation time.

### 3.1.2. Zeta-potential measurements

The system based on HA and PVA-SbQ starts from a homogonous solution. Also it is related to the relative concentrations and the colloid with micellar structure is obtained when the concentration of the HA/PVA-SbQ composites solution is low.

Fig. 1D depicts the dependence of the Zeta-potential of HA, PVA-SbQ and HA/PVA-SbQ composite solutions. It is seen that zeta-values of HA and HA/PVA-SbQ complex micelles are negative and zeta-value of PVA-SbQ is positive, which confirms that the shell moieties of the HA/PVA-SbQ complex micelles contain $-COO^-$ groups. The change in the value of the zeta-potential of HA/PVA-SbQ complex micelles, compared with that of HA, is due to the binding of additional positively charged PVA-SbQ molecules to the HA chains. This change means that some negative charges from HA were neutralized with the addition of PVA-SbQ, while the rest of the carboxylate groups provided net negative charges for the HA/PVA-SbQ complex micelles.

### 3.1.3. TEM

To visualize the HA/PVA-SbQ complex micelles, TEM image (Fig. 1E: c) was obtained. TEM images of HA and PVA-SbQ aggregates (Fig. 1E: a, b) were also obtained for the comparison. As shown in Fig. 1E, the typical core-shell type micellar aggregates in HA and PVA-SbQ solution were not found, while tight core-shell type micellar aggregates with an average diameter of around 462 nm were found in HA/PVA-SbQ composite solution. The spherical morphology of the micelles probably results from the presence of hydrophobic interactions among the SbQ molecules of PVA-SbQ and the presence of excess negative charges on the HA chain. The hydrophobic species form the micellar core, while HA with the negative charges provides the stabilization commonly encountered in small molecule SbQ and forms the micellar shell.

### 3.1.4. UV–vis spectroscopy

UV–vis spectroscopy was utilized to trace the photo-crosslinked process of HA/PVA-SbQ composite solution. The UV absorption spectra of the HA/PVA-SbQ composite solution at with different irradiation time are shown in Fig. 2a. When HA/PVA-SbQ solutions were exposed to 200–800 nm light in measurement, dramatically absorption bands occur at 340 nm for HA/PVA-SbQ composite solution with different UV irradiation time which can be attributed to the presence of the SbQ group on the PVA backbone. As shown in Fig. 2b, c, the absorbance intensity at around 340 nm decreased sharply and photo-dimerization degree increased significantly with increasing the irradiation time, indicating the dimerization of SbQ moieties. UV irradiation is assumed to result in the formation of cyclobutane rings which leads to the crosslinking of the PVA chains (see Scheme 1) and consequently HA/PVA-SbQ solutions show higher elastic system. This is consistent with the result of rheological analysis. Ichimura et al. reported that the photosensitivity of PVA-SbQ was high in spite of the extraordinarily low content of the styrylpyridinium group (Ichimura, 1996).

### 3.1.5. DLS

Fig. 3 shows the correlation function $g^1(t)$ for the PVA-SbQ solution and HA/PVA-SbQ composite solution and the corresponding hydrodynamic radius $R_h$ distribution $f(R_h)$ and effect of irradiation time on $R_h$ of HA/PVA-SbQ composite solutions.$g^1(t)$ is a normalized

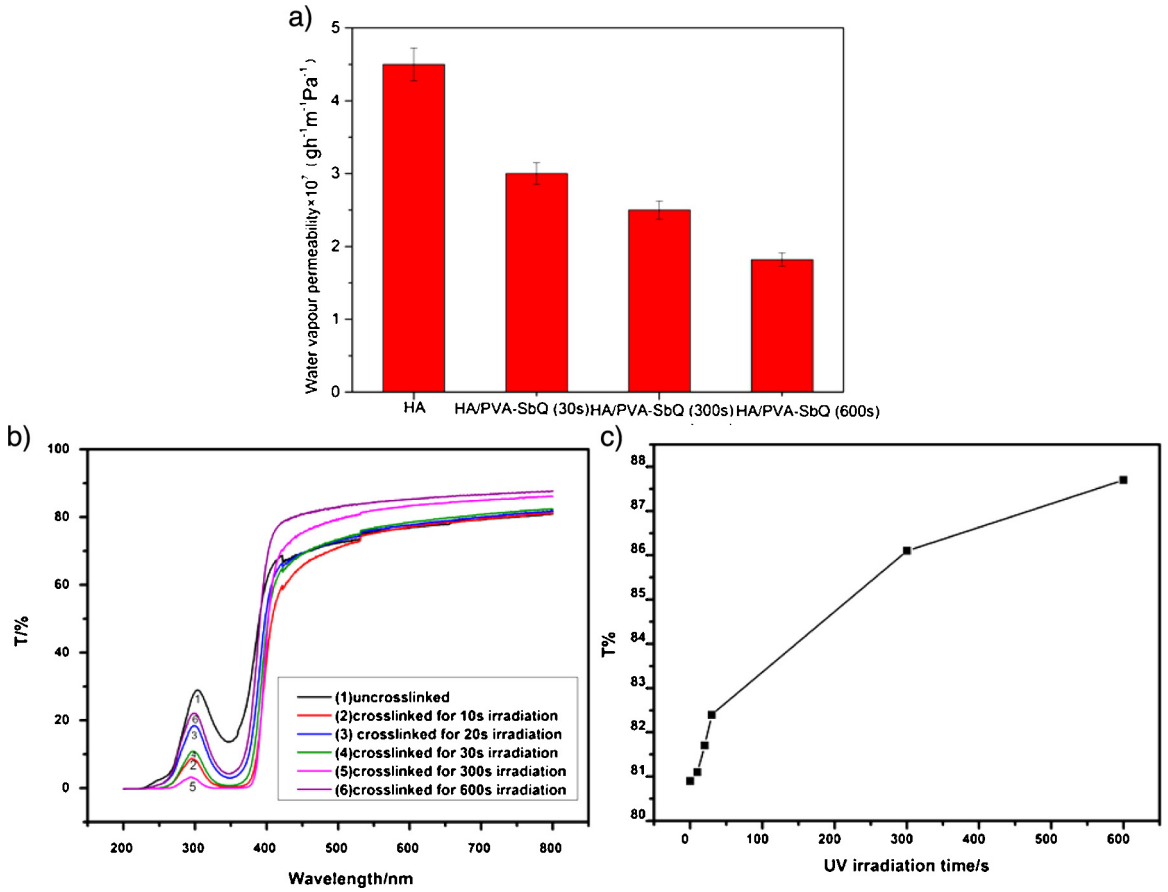


**Fig. 6.** Water vapor permeability (WVP) values (a) of the pure HA and HA/PVA-SbQ composite films with different UV irradiation time (30, 300, 600 s) and the optical transmittance (b), and the visible light transparency (c) of HA/PVA-SbQ composites films with different UV irradiation time.

scattered electric field-field time correlation function. In practice, the "normalized" correlation function is usually analyzed. Usually, the hydrodynamic radius $R_h$ is determined by analyzing $g^1(t)$ (Wu, 1993). Some researchers developed this method for the analysis of a gelation process of polymeric systems (Boyko & Richter, 2004; Richter, Boyko, Matzker, & Schröter, 2004; Richter, Matzker, & Schröter, 2005; Takata, Norisuye, Tanaka, & Shibayama, 2000) and the micellization of block ionomer microreactors containing different metal ions (Moffitt & Eisenberg, 1997). As shown in Fig. 3a, the $g^1(t)$ for the PVA-SbQ solution and HA/PVA-SbQ composite solution were similar to the typical measured $g^1(t)$ of polystyrene in toluene (Wu, 1993).

As shown in Fig. 3b, the HA/PVA-SbQ composite aggregate has a wider $f(R_h)$ than the pure PVA-SbQ aggregate. It is due to the HA providing the small $R_h$ and SbQ molecules of PVA-SbQ with benzene ring and pyridine ring providing the big $R_h$. To investigate the photo-crosslinking process more intensively, the sizes of HA/PVA-SbQ composite solutions after UV irradiation were monitored by using an ALV-5000/E dynamic light scattering instrument.

As shown in Fig. 3c, the $R_h$ of HA/PVA-SbQ composite aggregate decreases gradually as the UV irradiation time increases and the $R_h$ value decreased from 231 nm (the initial value) to 158 nm when being exposed to UV light for 15 min. As discussed above (Section 3.1.4, Fig. 2), the HA/PVA-SbQ composite can be photo-crosslinked because of the photodimerization of SbQ. Photo-crosslinking induced shrinkage of micelle particles, leading to the decrease of $R_h$ value (Jiang, Qi, Lepage, & Zhao, 2007; Liu et al., 2010; Xu et al., 2011). In our previous study, HA undergoes degradation which can also result in the decrease of $R_h$ value. As the same control experiment, the $R_h$ value of pure HA was measured after different UV irradiation time and the size of pure HA decrease from 90 to 71 nm (Xu et al., 2011). It is a much smaller change compared to that of HA/PVA-SbQ composite. Therefore, the decrease of the size of HA/PVA-SbQ composite should be mainly attributed to the crosslinking of composite.

### 3.2. Properties and characterization of HA/PVA-SbQ composites films

#### 3.2.1. Mechanical properties of HA/PVA-SbQ composites films

Mechanical properties evaluated in present study were tensile strength (TS) and elongation at break (EB). TS is a measure of film strength, whereas EB is a measure of film stretchability prior to breakage. Both properties are important in evaluation of packaging materials. Fig. 4(A–C) shows the stress–strain properties of HA/PVA-SbQ composites films and the effect of UV irradiation time on the tensile strength and elongation at break. As shown in Fig. 4(B, C), compared with the control film, the crosslinked specimens showed a higher TS but a lower EB. TS of the composites films has a trend of increase with the increase of UV irradiation time, and the maximum value achieved 71.0 MPa (see Fig. 4(B)). EB of composites films was about 5.4% of average (see Fig. 4(C)). The enhancement in TS of composites films may have been attributed to the fact the photodimerization of SbQ resulted in the crosslinking interactions of composites. Mechanical properties are largely associated with distribution and density of intermolecular interactions in the network. The tensile strength results are in close accordance with the rheological results given above. The values of TS exhibited by HA/PVA-SbQ composites films were of the same trend of storage modulus ($G'$) shown by HA/PVA-SbQ composite

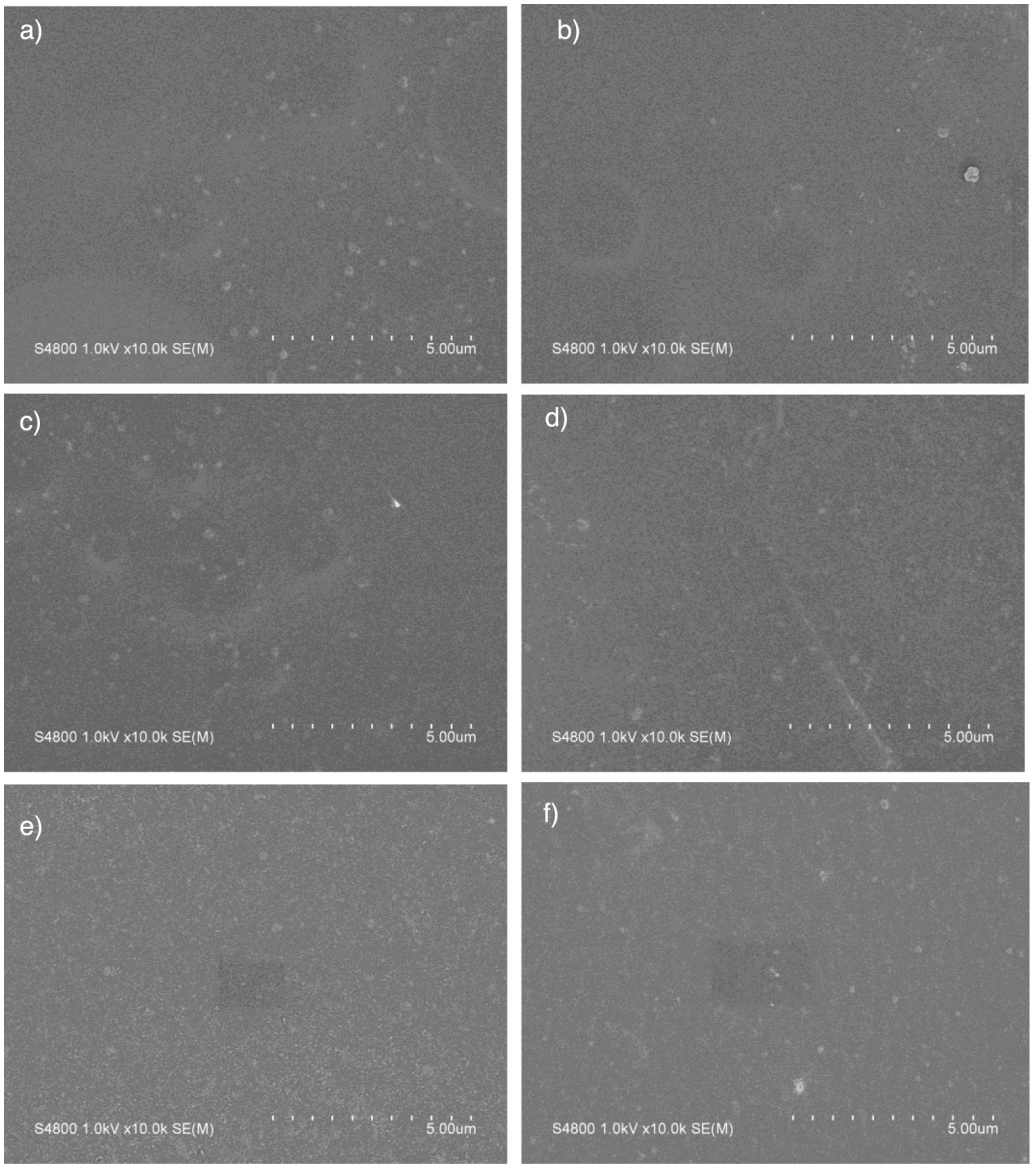


**Fig. 7.** SEM micrographs of HA/PVA-SbQ composites films with different UV irradiation time (a: 0, b: 10, c: 20, d: 30, e: 300, f: 600 s).

solutions. These results suggest that photo-crosslinking is a better method for improving the mechanical properties of HA/PVA-SbQ composite films by increasing TS while retaining a greater EB than uncrosslinked HA/PVA-SbQ composite films. Overall, HA/PVA-SbQ composite films have very attractive mechanical properties.

### 3.2.2. *Thermal properties of HA/PVA-SbQ composites films*

Fig. 5A shows the DSC thermograms for the HA/PVA-SbQ composite solution radiated at different irradiation time. As shown in Fig. 5A, all of the samples showed the presence of a broad endothermic peak around 100 °C, which is associated with the loss of moisture remaining after the initial drying procedure. Significant sharp exothermic peaks were also observed for each sample at higher temperatures (around 240 °C) and UV photo-crosslinking influences the relative magnitude of these two exothermic peaks. It is thought that the first of these peaks represents conversion into a less-ordered state, and the second of these peaks represents thermal degradation. As shown in Fig. 5A, as for the first peaks, they had no significant change with the UV irradiation time. In order to understand the change in order structure of HA/PVA-SbQ films further, XRD was used to describe the order phase of HA/PVA-SbQ films in the following section. As the second peaks, they had higher temperature shift slightly with the UV irradiation time. These indicated that the less-ordered structure of the crosslinked HA/PVA-SbQ films was formed and thermal stability of HA/PVA-SbQ films was improved due to the crosslinking reaction of the PVA-SbQ. Similar phenomena were observed in study on electrodeposition of hyaluronic acid and composite films (Sun & Zhitomirsky, 2009) and physical properties of crosslinked hyaluronic acid hydrogels (Collins & Birkinshaw, 2008).

### 3.2.3. *XRD*

As shown in Fig. 5B(a, b), X-ray scans of HA/PVA-SbQ composites films with different UV irradiation time show a weak peak at $2\theta = 25^\circ$ related to hyaluronic acid (Abdel-Mohsen et al., 2012) and two strong peaks at $2\theta = 17^\circ$ and $14^\circ$ related to PVA (Mahmoud, Al-Ghamdi, & Kadi, 2012). The UV irradiation for HA/PVA-SbQ composites films resulted in the decrease in peaks intensity and the decrease trends of peaks intensity were observed with increasing UV irradiation time, showing the destruction of the ordered phase or an increase in amorphous content of HA/PVA-SbQ composites films. This is due to photo-crosslinking interaction of HA/PVA-SbQ

composites that disrupts the regularity of the chain structures in HA and PVA-SbQ and increases the spacing between the chains.

### 3.2.4. Water vapor barrier properties of HA/PVA-SbQ composites films

Water vapor permeability (WVP) was investigated to understand the effect of UV irradiation on water vapor barrier properties of HA/PVA-SbQ composites films. Fig. 6a shows WVP values of pure HA and HA/PVA-SbQ composites films with different UV irradiation time (30, 300, 600 s). As shown in Fig. 6a, WVP data were in the range $(1.82–4.5) \times 10^{-7}$ g/(m h Pa)$^{-1}$ and were significantly affected by UV irradiation time for HA/PVA-SbQ composite films. WVP values decreased with increasing UV irradiation time. In particular, HA/PVA-SbQ composite film with 600 s had WVP value $1.82 \times 10^{-7}$ g/(m h Pa)$^{-1}$ which is 59% lower than the value of pure HA, indicating that UV irradiation greatly reduced the WVP of HA/PVA-SbQ composite films. These results might be attributed to the network formed by both photodimerization of SbQ of PVA-SbQ and hydrogen reaction between hydroxyls groups of PVA-SbQ and carboxyl of hyaluronic acid in HA/PVA-SbQ composites. This network reduces the free volumes of the HA/PVA-SbQ composite films and increases the tortuosity of the water molecules pathway through these films. With the consequent the decrease in WVP is obtained. Many studies also indicate that water vapor permeation process is controlled by the diffusion of water through the film (Kristo & Biliaderis, 2007; Slavutsky & Bertuzzi, 2012, 2014). The addition of rigid crystalline structures produces a tortuous path that hinders the passage of water molecules through the film matrix. The longer diffusive path that the penetrant molecules must travel, leads to the reduction of permeability (Sihna Ray & Okamoto, 2003). In general, water vapor permeability presented in this work is lower than the values reported by other authors for the chitosan-HA material (Xu, Ma, Shi, Gao, & Han, 2007).

### 3.2.5. Optical properties

To investigate the effect of UV irradiation time on optical properties of HA/PVA-SbQ composites films, the optical transmittance of films were performed with UV–vis spectroscopy. It can be seen from Fig. 6(b) that the crosslinked HA/PVA-SbQ composites films shows not only higher UV light shielding but also higher visible light transparency than uncrosslinked HA/PVA-SbQ composites films. This agrees with the transmittance result (Fig. 2(a)). The results were due to photodimerization of SbQ of PVA-SbQ. Generally, transparency of films is also an auxiliary criterion to judge the miscibility of two or more polymer-mixed films (Li & Xie, 2004). The optical transmittance ($T$ %) dependence of the wavelength (200–800 nm) for HA/PVA-SbQ composites films with different UV irradiation time is shown in Fig. 6(b). As shown in Fig. 6(c), with the increase in UV irradiation time, the crosslinking interaction of composites strengthened, and the transparency increased, indicating good miscibility between HA and PVA-SbQ. So HA/PVA-SbQ composites films with high-UV light shielding efficiency and high-visible light transparency are suitable for transparent packaging materials.

### 3.2.6. SEM

It is necessary to study the morphology of the polymer blends since their mechanical properties depend on it. SEM micrographs of HA/PVA-SbQ composites films with different UV irradiation time were presented in Fig. 7. Compared the morphology of HA/PVA-SbQ composites films with shorter UV irradiation time (Fig. 7(a–d)), the films with longer UV irradiation time (Fig. 7(e, f)) can be found that the size of dispersion phase decreases, showing that there is a fine dispersion and homogeneity of PVA-SbQ in the HA. This better dispersion arises from the formation of crosslinked macromolecules that is due to photodimerization of SbQ of PVA-SbQ and hydrogen reaction between hydroxyls groups of PVA-SbQ and carboxyl of hyaluronic acid. Thus the interfacial tension between the two polymers was reduced and a finer distribution of PVA-SbQ in the HA was observed.

## 4. Conclusions

In this study, we reported the rheological and structural characterization of a novel photo-crosslinkable HA/PVA-SbQ composite film-forming solution and films from HA and PVA-SbQ with different UV irradiation time. On application of dynamic rheological tests, all film-forming solutions showed physical gel-like behavior. The self-assembly behavior in aqueous solution and structural of HA/PVA-SbQ complex micelles were investigated. The strong association between HA and PVA-SbQ is driven by electrostatic attraction and the hydrophobic interactions between SbQ moieties. During the self-assembly process, core-shell type nano-sized micellar aggregates were observed, as characterized by TEM, zeta potential measurements and DLS. UV spectra and DLS analysis confirmed that the micelles were photo-crosslinkable and that the photo-crosslinking of the inner core led to a decrease in size of the micelle particles. The effect of UV irradiation times on the mechanical and thermal and water vapor barrier as well as optical properties of HA/PVA-SbQ composite films was studied. The results show that photo-crosslinking increases TS and retains a greater EB than uncrosslinked HA/PVA-SbQ composite films. The crosslinked HA/PVA-SbQ composite films exhibited high optical transparence and improved thermal stability and water vapor barrier property. X-ray diffraction patterns of HA/PVA-SbQ composite films confirmed the ordered phase was destructed with UV irradiation time. SEM images indicated that there is a fine dispersion and homogeneity of PVA-SbQ in the HA for the crosslinked HA/PVA-SbQ composite films with longer UV irradiation time.

The HA/PVA-SbQ composite films were safe and biodegradable, therefore have a potential application as packaging materials. The methods investigated and developed in this study are expected to be very useful for future research in developing edible films.

## Acknowledgements

This work was supported by the National Science Foundation of China (grant no. 51373070) and the Fundamental Research Funds for the Central Universities (JUSRP21112) as well as the MOE & SAFEA for the 111 Project (B13025).

## References

Ambrosio, L., Borzacchiello, A., Netti, P. A., & Nicolais, L. J. (1999). Rheological study on hyaluronic acid its derivative solutions. *Journal of Macromolecular Science, Part A: Pure and Applied Chemistry*, *A36*, 991.

Abdel-Mohsen, A. M., Hrdina, R., Burgert, L., Krylová, G., Abdel-Rahman, R. M., Krejčová, A., et al. (2012). Green synthesis of hyaluronan fibers with silver nanoparticles. *Carbohydrate Polymers*, *89*, 411–422.

Barbucci, R., Borzacchiellob, A., Ambrosiob, L., Finic, M., Torricellic, P., & Giardinoc, R. (2002). Hyaluronic acid hydrogel in the treatment of osteoarthritis. *Biomaterials*, *23*, 4503–4513.

Boyko, V., & Richter, S. (2004). Monitoring of the gelation process on a radical chain cross-linking reaction based on N-vinylcaprolactam by using dynamic light scattering. *Macromolecular Chemistry and Physics*, *205*, 724–730.

Bulpitt, P., & Aeschlimann, D. (1999). New strategy for chemical modification of hyaluronic acid: Preparation of functionalized derivatives and their use in the formation of novel biocompatible hydrogels. *Journal of Biomedical Materials Research Part A*, *47*, 152–169.

Cuq, B., Aymard, C., Cuq, J. L., & Guilbert, S. (1995). Edible packaging films based on fish myofibrillar proteins: Formulation and functional properties. *Journal of Food Science*, *60*, 1369–1374.

Cockburn, E. S., Davidson, R. S., & Pratt, J. E. (1996). The photocrosslinking of styrylpyridinium salts via a [2 + 2]-cycloaddition reaction. *Journal of Photochemistry and Photobiology A*, *94*, 83–88.

Chamberlain, E. K., & Rao, M. A. (2000). Effect of concentration on rheological properties of acid-hydrolyzed amylopectin solutions. *Food Hydrocolloids*, *14*, 163–167.

Cowman, M. K., & Matsuoka, S. (2005). Experimental approaches to hyaluronan structure. *Carbohydrate Research*, *340*, 791–809.

Collins, M. N., & Birkinshaw, C. (2008). Physical properties of crosslinked hyaluronic acid hydrogels. *Journal of Materials Science: Materials in Medicine*, *19*, 3335–3343.
Chytil, M., & Pekar, M. (2009). Effect of new hydrophobic modification of hyaluronan on its solution properties: Evaluation of self-aggregation. *Carbohydrate Polymers*, *76*, 443–448.
Gao, H. J., Du, G. C., & Chen, J. (2006). Analysis of metabolic fluxes for hyaluronic acid (HA) production by streptococcus zooepidemicus. *World Journal of Microbiology and Biotechnology*, *22*, 399–408.
Ghasemlou, M., Khodaiyan, F., & Oromiehie, A. (2011). Rheological and structural characterisation of film-forming solutions and biodegradable edible film made from kefiran as affected by various plasticizer types. *International Journal of Biological Macromolecules*, *49*, 814–821.
Hertzberg, S., Moen, E., Vogelsang, C., & Østgaard, K. (1995). Mixed photo-cross-linked polyvinyl alcohol and calcium-alginate gels for cell entrapment. *Applied Microbiology and Biotechnology*, *43*, 10–17.
Ichimura, K., & Watanabe, S. (1980). Highly photosensitive polymers with anomalously low content of stilbazolium groups. *Journal of Polymer Science: Polymer Letters Edition*, *18*, 613–617.
Ichimura, K., & Watanabe, S. (1982). Preparation and characteristics of photocross-linkable poly (vinyl alcohol). *Journal of Polymer Science: Polymer Chemistry Edition*, *20*, 1419–1432.
Ichimura, K. (1996). Photocrosslinkable poly(vinyl alcohols): Preparation, properties and applications. *Heterogeneous Chemistry Reviews*, *3*, 419–441.
Jiang, J. Q., Qi, B., Lepage, M., & Zhao, Y. (2007). Polymer micelles stabilization on demand through reversible photo-cross-linking. *Macromolecules*, *40*, 790–792.
Kristo, E., & Biliaderis, C. (2007). Physical properties of starch nanocrystal-reinforcedpullulan films. *Carbohydrate Polymers*, *68*, 146–158.
Luo, Y., Kirker, K. R., & Prestwich, G. D. (2000). Cross-linked hyaluronic acid hydrogel films: New biomaterials for drug delivery. *Journal of Controlled Release*, *69*, 169–184.
Li, B., & Xie, B. J. (2004). Synthesis and characterization of konjac glucomannan/poly(vinyl alcohol) interpenetrating polymer networks. *Journal of Applied Polymer Science*, *93*, 2775–2780.
Lafargue, D., Lourdin, D., & Doublier, J.-L. (2007). Film-forming properties of a modified starch/κ-carrageenan mixture in relation to its rheological behaviour. *Carbohydrate Polymers*, *70*, 101–111.
Lee, H., Lee, K., & Park, T. G. (2008). Hyaluronic acid–paclitaxel conjugate micelles: Synthesis, characterization, and antitumor activity. *Bioconjugate Chemistry*, *19*, 1319–1325.
Lee, H., Ahn, C. H., & Park, T. G. (2009). Poly[lactic-co-(glycolic acid)]-grafted hyaluronic acid copolymer micelle nanoparticles for target-specific delivery of doxorubicin. *Macromolecular Bioscience*, *9*, 336–342.
Liu, Y., Bolger, B., Cahill, P. A., & McGuinness, G. B. (2009). Water resistance of photocrosslinked polyvinyl alcohol based fibers. *Materials Letters*, *63*, 419–421.
Liu, X. Y., Yi, C. L., Zhu, Y., Yang, Y. Q., Jiang, J. Q., & Cui, Z. G. (2010). Pickering emulsions stabilized by self-assembled colloidal particles of copolymers of P(St-alt-MAn)-co-P(VM-alt-MAn). *Journal of Colloid and Interface Science*, *351*, 315–322.
Moffitt, M., & Eisenberg, A. (1997). Scaling relations and size control of block ionomer microreactors containing different metal ions. *Macromolecules*, *30*, 4363–4373.
Moraes, I. C. F., Carvalho, R. A., Bittante, A. M. Q. B., Solorza-Feria, J., & Sobral, P. J. A. (2009). Film forming solutions based on gelatin and poly(vinyl alcohol) blends: Thermal and rheological characterizations. *Journal of Food Engineering*, *95*, 588–596.
Mahmoud, W. E., Al-Ghamdi, A. A., & Kadi, M. W. (2012). The influence of γ-rays irradiation on the structure and crystallinity of heteropoly acid doped PVA. *Radiation Physics and Chemistry*, *81*, 693–696.
Ogrodowski, C. S., Hokka, C. O., & Santana, M. H. (2005). Production of hyaluronic acid by streptococcus. *Applied Biochemistry and Biotechnology*, *121–124*, 753–761.
Ou, S. Y., Kwok, K. C., & Kang, Y. J. (2004). Changes in vitro digestibility and available lysine of soy protein isolate after formation of film. *Journal of Food Engineering*, *64*, 301–305.
Peressini, D., Bravin, B., Lapasin, R., Rizzotti, C., & Sensidoni, A. (2003). Starch-methylcellulose based edible films: Rheological properties of film-forming dispersions. *Journal of Food Engineering*, *59*, 25–32.
Pitarresi, G., Pierro, P., Palumbo, F. S., Tripodo, G., & Giammona, G. (2006). Photocross-linked hydrogels with polysaccharide-poly(amino acid) structure: New biomaterials for pharmaceutical applications. *Biomacromolecules*, *7*, 1302–1310.
Pires, A. M. B., & Santana, M. H. A. (2011). Rheological aspects of microbial hyaluronic acid. *Journal of Applied Polymer Science*, *122*, 126–133.
Richter, S., Boyko, V., Matzker, R., & Schröter, K. (2004). Gelation studies: Comparison of the critical exponents obtained by dynamic light scattering and rheology: 2. A thermoreversible gelling system: Mixtures of xanthan gum and locust-bean gum. *Macromolecular Rapid Communications*, *25*, 1504–1509.
Richter, S., Matzker, R., & Schröter, K. (2005). Gelation studies, 4 why do "classical" methods like oscillatory shear rheology and dynamic light scattering for characterization of the gelation threshold sometimes not provide identical results especially on thermoreversible gels? *Macromolecular Rapid Communications*, *26*, 1626–1632.
Rinaudo, M. (2008a). Rheological investigation on hyaluronan-fibrinogen interaction. *International Journal of Biological Macromolecules*, *43*, 444–450.
Rinaudo, M. (2008b). Main properties and current applications of some polysaccharides as biomaterials. *Polymer International*, *57*, 397–430.
Rwei, S. P., Chen, S. W., Mao, C. F., & Fang, H. W. (2008). Viscoelasticity and wearability of hyaluronate solutions. *Biochemical Engineering Journal*, *40*, 211–217.
Shindo, Y., Morikawa, S., Hasegawa, M., Sugimura, T., & Adachi, D. (1995). Photocrosslinking reaction and dynamic viscoelastic properties of photosensitive poly (vinyl alcohol). *Journal of Photopolymer Science and Technology*, *8*, 125–128.
Shindo, Y., Hasegawa, M., Kawanobe, J., & Inoue, K. (2001). Water resistance of photosensitive poly(vinyl alcohol) films. *Journal of photopolymer science and technology*, *14*, 293–294.
Shindo, Y., Yamada, Y., Kawanobe, J., & Inoue, K. (2002). Reactivities and thermal mechanical properties of poly(vinyl alcohol) and poly(vinyl-b-acrylic acid) with pendant styrylpyridinium groups. *Journal of Photopolymer Science and Technology*, *15*, 153–158.
Sihna Ray, S., & Okamoto, M. (2003). Polymer/layered silicate nanocomposites: A review from preparation to processing. *Progress in Polymer Science*, *28*, 1539–1641.
Slavutsky, A. M., & Bertuzzi, M. A. (2012). A phenomenological and thermodynamic study of the water permeation process in corn starch/MMT films. *Carbohydrate Polymers*, *90*, 551–557.
Slavutsky, A. M., & Bertuzzi, M. A. (2014). Water barrier properties of starch films reinforced with cellulose nanocrystals obtained from sugarcane bagasse. *Carbohydrate Polymers*, *110*, 53–61.
Sun, F., & Zhitomirsky, I. (2009). Electrodeposition of hyaluronic acid and composite films. *Surface Engineering*, *25*, 621–627.
Takata, S., Norisuye, T., Tanaka, N., & Shibayama, M. (2000). Heat-induced gelation of β-lactoglobulin. 1. Time-resolved dynamic light scattering. *Macromolecules*, *33*, 5470–5475.
Tao, Y. H., Ai, L., Bai, H. Y., & Liu, X. Y. (2012). Synthesis of pH-responsive photocrosslinked hyaluronic acid-based hydrogels for drug delivery. *Journal of Polymer Science Part A: Polymer Chemistry*, *50*, 3507–3516.
Tomé, L. C., Goncalves, C. M. B., Boaventura, M., Brandão, L., Mendes, A. M., Silvestre, A. J. D., et al. (2011). Preparation and evaluation of the barrier properties of cellophane membranes modified with fatty acids. *Carbohydrate Polymers*, *83*, 836–842.
Vázquez, C. P., Boudou, T., Dulong, V., Nicolas, C., Picart, C., & Glinel, K. (2009). Variation of polyelectrolyte film stiffness by photo-cross-linking: A new way to control cell adhesion. *Langmuir*, *25*, 3556–3563.
Wu, C. (1993). An alternative way to analyze quasi-elastic light scattering data for broadly distributed samples. *Colloid and Polymer Science*, *271*, 947–951.
Xu, H. T., Ma, L., Shi, H. F., Gao, C. Y., & Han, C. M. (2007). Chitosan–hyaluronic acid hybrid film as a novel wound dressing: In vitro and in vivo studies. *Polymers for Advanced Technologies*, *18*, 869–875.
Xu, J., Bai, H. Y., Yi, C. L., Luo, J., Yang, C., Xia, W. S., et al. (2011). Self-assembly behavior between native hyaluronan and styrylpyridinium in aqueous solution. *Carbohydrate Polymers*, *86*, 678–683.
Xu, X., Liu, W., & Zhang, L. (2006). Rheological behavior of aeromonas gum in aqueous solutions. *Food Hydrocolloids*, *20*, 723–729.